Tuijin Jishu/Journal of Propulsion Technology
ISSN: 1001-4055
Vol. 44 No. 5 (2023)

An Advanced Formulation for Rehabilitating Shear Strength in Deep Beams with Shear Openings through Integration of Varied Steel Configurations for Utility Provisions

[1]Prachi G. Shah, [2]Nirpex A. Patel, [3]Vijay R. Panchal

[1]M. S. Patel Department of Civil Engineering, Chandubhai S. Patel Institute of Technology, Charotar University of Science and Technology, Changa, Gujarat, India

[2][3] M. S. Patel Department of Civil Engineering, Chandubhai S. Patel Institute of Technology, Charotar University of Science and Technology, Changa, Gujarat, India

Abstract—In the contemporary urban landscape, rapid technological advancements necessitate adaptations in industrial and residential structures to accommodate new utilities such as ducts, pipes, and passages. This study focuses on formulating a design methodology and aid for recovering shear capacity losses resulting from openings in existing solid deep beams. A novel design approach involves the implementation of steel elementary configurations around the openings in deep beams, enhancing their shear resistance. The study employs a systematic investigation, integrating simulation through the ABAQUS program, to assess the effectiveness of the proposed steel configurations in restoring shear capacity. The research explores three distinct steel configurations, emphasizing the synergy between concrete and steel materials. Concrete Damage Plasticity models, incorporated within ABAQUS, enable detailed quasi-static analysis to unravel the intricate behaviour of deep beams subjected to shear openings and strengthened with proposed steel formations. Specifically, a deep beam model featuring a combination of a full-length steel plate welded with a steel cylinder around the opening (EDSBPD) exhibited full capacity restoration, achieving an efficiency of 1.0064 compared to solid deep beams. Leveraging ABAQUS simulations and adhering to ACI 318-14 specifications, a parametric study was conducted to investigate the EDSBPD for design assistance. This study led to the development of a dimensionless equation that calculates the shear strength of deep beams, accounting for the impact of the thickness-to-width ratio of the steel configuration around the opening. This equation provides a valuable tool for incorporating openings into solid deep beams without compromising shear strength.

Index Terms—Deep beam, Proposed configuration, opening to shear zone, Finite Element Modelling, Concrete damaged plasticity, Prediction of shear strength, ABAQUS

ABBREVIATION AND NOMENCLATURE

DEO	Extra reinforcement provided on top and bottom adjacent sides of the opening
OEB	Opening provided to existing solid deep beam
EDSPO	Steel plates with bolts provided on top and bottom adjacent sides of opening
EDSBPB	Steel cylinder accompanied plates assembled around opening with the help of bolts
EDSBPD	Full-length steel plate accompanied steel cylinder around the opening
E_0	Young's modulus
σ_t	Tensile stress
σ_c	Compressive stress
d_t	Damage parameter for tension
d_c	Damage parameter for compression
σ_{t0}	Cracking stress of concrete.
ε_{cr}	Cracking strain of concrete.

1. INTRODUCTION

In the contemporary construction landscape, the need to accommodate diverse essential services like air-conditioning ducts, sanitation, and various wiring systems within existing structures necessitates the introduction of openings in structural elements. However, this modification poses challenges as it impacts the load-carrying capacity significantly. Extensive research has been conducted to fortify beams and columns with openings, focusing on non-linear stress distribution analysis and preventive measures against capacity loss after core cutting. To address this, external steel configurations are proposed and systematically studied through a parametric analysis to develop a viable provision formula.

ECP 203-2007 guidelines specify parameters for deep beams with a shear span-to-depth ratio ≤ 2 and clear span-to-height ratio of four. Reinforcement distribution should ideally fall between 0.1 to 0.2 times the beam depth.

ACI 318-14 outlines the strut-and-tie method for designing solid deep beams, emphasizing force equilibrium in a chosen truss model rather than traditional beam theory, especially for shallow beams.

Previous research concentrated upon studying the effect of opening on the shear capacity of the deep beam such as;

Ibrahim et al. [1] and [6] proposed that shear and flexure capacities in a beam are approximately equal, with openings reducing capacity by up to 50%.

Mohamed et al. [3] employed Finite Element Analysis (FEA) to study load capacity and behavior, conducting a parametric study to optimize reinforcement distribution and determine the maximum depth of openings relative to beam depth.

Hafezolghorani [4] introduced mathematical examples for analyzing the non-linear behavior of reinforced concrete elements.

Bose et al. [7] identified failure causes in various beam types, emphasizing shear failure in deep beams. Yang et al. [15] elucidated the impact of web openings on the structural response of reinforced high-strength concrete deep beams.

Campione and Minafò [11] investigated circular openings' effects, deriving equations to assess transverse tension in reinforced/unreinforced concrete struts.

El-Demerdash [12] verified experimental results through FEA using ANSYS program, enhancing understanding through computational analysis.

ECP 203-2007 [8] introduced guidelines of deep beam with shear span to depth ratio ≤ 2 and for beam with clear span is four times of its height. The range for reinforcement distribution should be 0.1 to 0.2 beam depth.

2. CONCRETE DAMAGED PLASTICITY (CDP) MODEL AND MATERIAL PROPERTIES.

In the analysis of High-Strength Concrete (HSC), a concrete model with a compressive strength of 53 MPa, as proposed by Ibrahim et al. [1], is utilized. The model incorporates two key hypotheses: compressive crushing and tensile cracking of concrete, forming the basis of a nonlinear concrete model. To account for damage parameters, the scalar damage assumption is applied, aligning with the properties of Concrete Damage Plasticity (CDP), well-illustrated by Grassl, P. et al. [9] and Wahalathantri B. L. et al. [2]. The evaluation of elastic and plastic properties is conducted following guidelines outlined in the ABAQUS analysis user's manual [5], with specific parameters detailed in Tables I and II for reference.

Table I: Concrete general properties

Density (tonne/mm^3)	Modulus of elasticity (MPa)	Poison's ratio
2.4e-09	31500	0.2

Table II: Concrete plasticity properties

Dilation angle	F_{bo}/f_{co}	Eccentricity	Viscosity parameter	K
38˚	1.16	0.1	0	0.67

A. Tension stiffening relationship for concrete

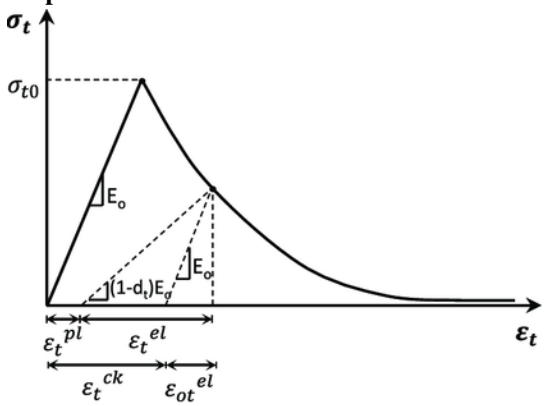

Figure 1:

Fig. 1 illustrates the definition of the tension stiffening model for concrete based on the stress-strain relation, sourced from the ABAQUS Analysis user's manual of 2016 [5].

The post-failure stress-strain relation can be determined by establishing the relationship between post-failure stresses σ_{t0} and cracking strain, ε_t^{ck}.

Cracking strain is defined as the total strain minus the elastic strain corresponding to the undamaged material, denoted as $\varepsilon_t^{ck} = \varepsilon_t - \varepsilon_{0t}^{el}$, where $\varepsilon_{0t}^{el} = \sigma_t / E_0$. This relationship is depicted in Fig. 1.

For modeling the tensile stress-strain curve in the ABAQUS program, the modified tension stiffening model developed by Nayal and Rasheed [13] and incorporated by Ibrahim et al. [1] was selected. This model, as illustrated in Fig. 2 and detailed in Table III, was applied to define the tensile stress-strain behavior within the ABAQUS simulation.

To comply with ABAQUS requirements, the tensile damage parameters need to be specified. The program translates the cracking strain values into plastic strain values using the relationship described (1).

$$\varepsilon_t^{pl} = \varepsilon_t^{ck} - \frac{d_t}{(1-d_t)} \frac{\sigma_t}{E_0} \quad (1)$$

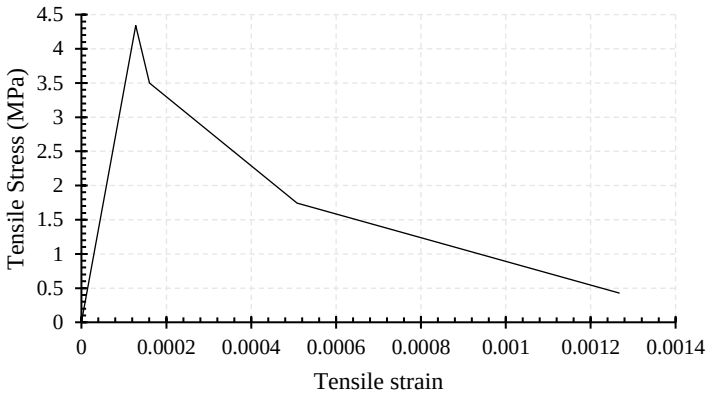

Fig 1: Definition of used tension stiffening for concrete in current study according to Nayal and Rasheed 2006 [13] and incorporated by Ibrahim et al. [1]

Table III: Tension stiffening of concrete for ABAQUS program in current study

Damage parameter	Cracking strain	Yield stress (MPa)	Cracking strain
0	0	4.3	0
0.66667	0.000507459	1.43333	0.000507459
0.9	0.002042082	0.215	0.002042082

B. Compression behavior for concrete

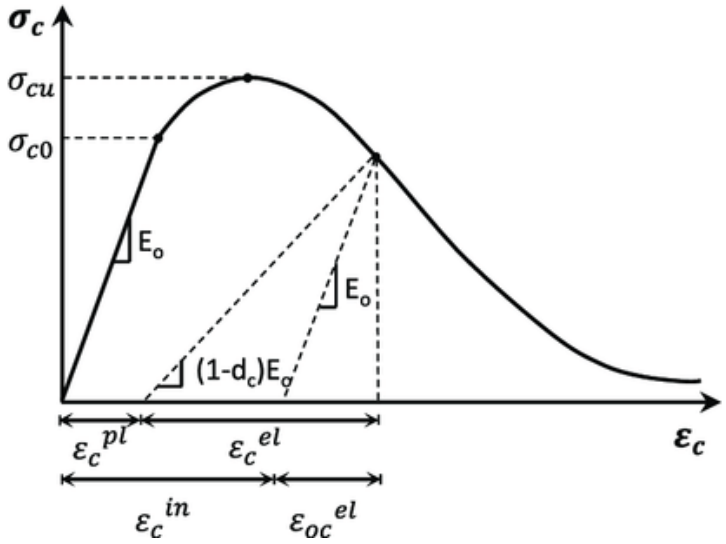

Fig. 3: presents the definition of concrete compression behavior in the ABAQUS analysis user's manual [5].

In this context, compression hardening data are specified in terms of inelastic strain ε_c^{in} rather than plastic strain ε_c^{pl}. The compressive inelastic strain is calculated as the total strain minus the elastic strain corresponding to the undamaged material, denoted as $\varepsilon_c^{in} = \varepsilon_c - \varepsilon_{0c}^{el}$, where $\varepsilon_{0c}^{el} = \sigma_c / E_0$. This relationship is visually depicted in Fig. 3 and further detailed in Fig. 4 and Table IV.

For ABAQUS analysis, it is essential to define the compressive damage parameters. The software automatically translates the crushing strain values into inelastic strain values using the relationship described (2).

$$\varepsilon_c^{pl} = \varepsilon_c^{in} - \frac{d_c}{(1-d_c)} \frac{\sigma_c}{E_0} \tag{2}$$

C. Modeling of stress-strain curve in compression for concrete

Hognestad [14] Model was chosen as follow:

Compressive stress at any point can be defined using (3) within range of 0 to ε_0 (strain at peak stress) which equals to, $\varepsilon_0 = \frac{2f'_c}{E_c}$.

Stress- strain relationship at any point from ε_0 to ε_{cu} can be obtained by (4)

$$\sigma_c = f'_c \left[2\frac{\varepsilon_c}{\varepsilon_0} - \left(\frac{\varepsilon_c}{\varepsilon_0}\right)^2\right] \qquad (\varepsilon_c \leq \varepsilon_0) \tag{3}$$

$$\sigma_c = f'_c \left[1 - 0.15\frac{\varepsilon_c - \varepsilon_0}{\varepsilon_c - \varepsilon_0}\right] \qquad (\varepsilon_0 < \varepsilon_c \leq \varepsilon_{cu}) \tag{4}$$

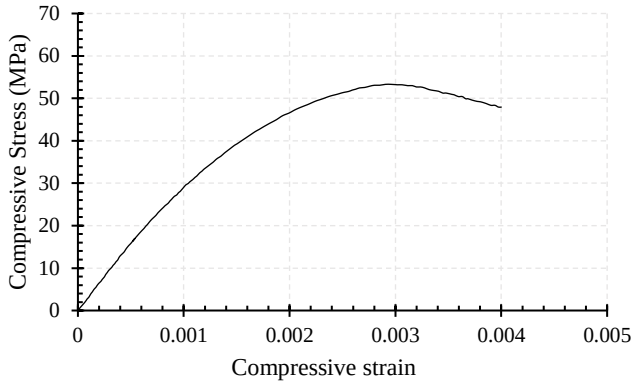

Fig 4: Compressive stress–strain relationship representing concrete in ABAQUS FE model after Hognestad [8] and incorporated by Ibrahim et al. [1]

Table IV: Compressive behavior of concrete for ABAQUS program in present study

Damage parameter	Inelastic strain	Yield stress (MPa)	Inelastic strain
0	0	31.5	0
0	0.0003535	36.0087441	0.0003535
0	0.0004668	44.3373587	0.0004668
0	0.0006327	50.7415632	0.0006327
0	0.0009041	53.3	0.0009041
0.0049407	0.0010158	53.0366581	0.0010158
0.0198225	0.0011421	52.2434625	0.0011421
0.044363	0.0012824	50.9354514	0.0012824
0.0777839	0.0014357	49.154116	0.0014357
0.1188649	0.0016002	46.9645013	0.0016002

D. Material properties for reinforcing steel in the FE model

The stress-strain relationship exhibits a bilinear isotropic elastic–perfectly plastic behavior for the rebar, demonstrating identical characteristics in both tension and compression, as illustrated in Fig. 5. The ABAQUS program incorporates specific elastic and plastic properties for steel reinforcements and steel shear devices, which are systematically outlined in Table V and VI.

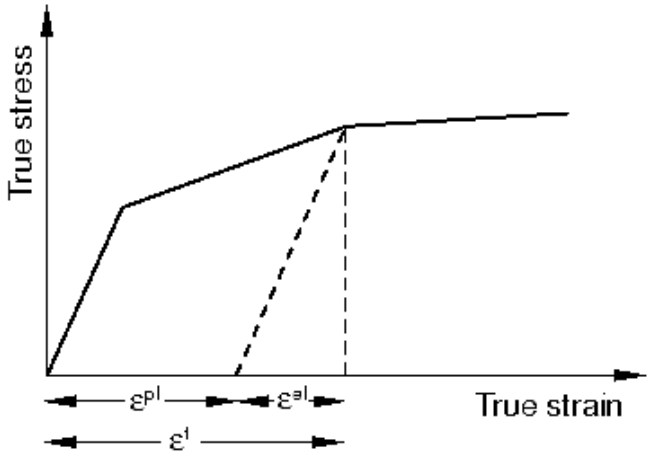

Fig 5: Definition of nominal stress-strain relationship for a uniaxial test of steel, ABAQUS analysis user's manual [5].

When nominal stress-strain data from a uniaxial test is accessible, and the material exhibits isotropic properties, a straightforward transformation to true stress σ_{true} and logarithmic plastic strain ε_{ln}^{pl} can be achieved using (5) and (6) respectively.

$$\sigma_{true} = \sigma_{nom}\,(1 + \varepsilon_{nom}) \quad (5)$$

$$\varepsilon_{ln}^{pl} = ln(1 + \varepsilon_{nom}) - \frac{\sigma_{true}}{E_0} \quad (6)$$

Table V: Mechanical properties of steel bars by Ibrahim et al. [10]

Bar diameter (mm)	C/S area (mm^2)	Yield strength (MPa)	Ultimate strength (MPa)	Elongation at failure (%)
6	28.3	371	577	37.6
8	50.29	324	464	35
10	78.5	536	638	24.3
12	113	560	692	18.9
16	201	512	640	22.4

Table VI: Mechanical properties of shear steel device

Density (tonne/mm^3)	Modulus of elasticity (MPa)	Poison's ratio	Yield stress (MPa)	Plastic strain
7.85e-09	210000	0.3	250	0

3. Validation of Present Study

Steel bars are modeled using 2-node linear 3D trusses (T3D2), while 8-node linear 3D bricks (C3D8R) elements are employed for steel plates and concrete components. Rebars are embedded within the concrete structure to account for the interaction between reinforcement and concrete material. A general contact interaction approach is implemented, utilizing surface-to-surface hard contact between consecutive surfaces of the loaded steel plates and concrete elements.

A parametric study is conducted to optimize the mesh size, leading to the selection of an ideal mesh size of 30mm. Displacement-based loading is applied in the simulation, with a maximum displacement of 5.5 mm introduced at reference points RP1 and RP2. The bottom surface of support plates is defined as ENCASTRE, representing a fully fixed boundary condition. Static loading is applied with a damping coefficient of 0.002, and the analysis is performed over a maximum of 1500 increments. The specific step increment range utilized in the analysis is detailed in Table VII.

Table VII: Model analysis step increments

Particulars	Initial	Least	Maximum
Increment size	0.01	1E-010	1

A. Mesh Sensitivity Analysis

Within the framework of this study, mesh sensitivity analysis serves as a vital component for validating the numerical simulations. This process entails methodically refining the computational mesh to assess its influence on the precision and stability of the outcomes. By systematically altering the mesh size within the range of 6000 to 22000 elements and monitoring efficiency variations (0.91 to 1.01) irrespective of meshing size of embedded reinforcements, the reliability of the finite element models is ensured as depicted in Fig. 6. Notably, the finite element model comprising 18,000 mesh elements exhibits an efficiency of approximately 100% concerning ultimate load capacity, aligning closely with FE model HMT in the findings of Ibrahim et al. [1]. This meticulously validated model is subsequently employed for further in-depth investigation.

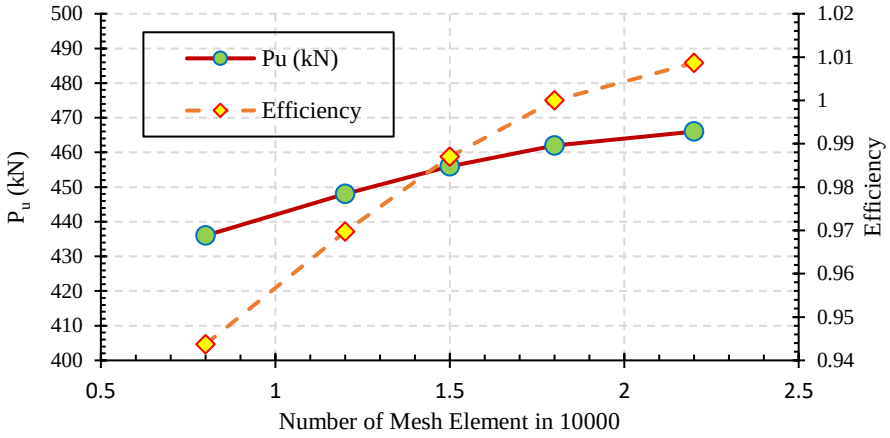

Fig 6: Mesh sensitivity analysis in accordance with CDP

B. Verification of FE model

For validation, a Detailed Engineering Order (DEO) is created following the specifications outlined in the study by Ibrahim et al. [1] for the HMT model. The design details and configurations depicted in Figures 7 and 8 are meticulously replicated and then compared against the reference model.

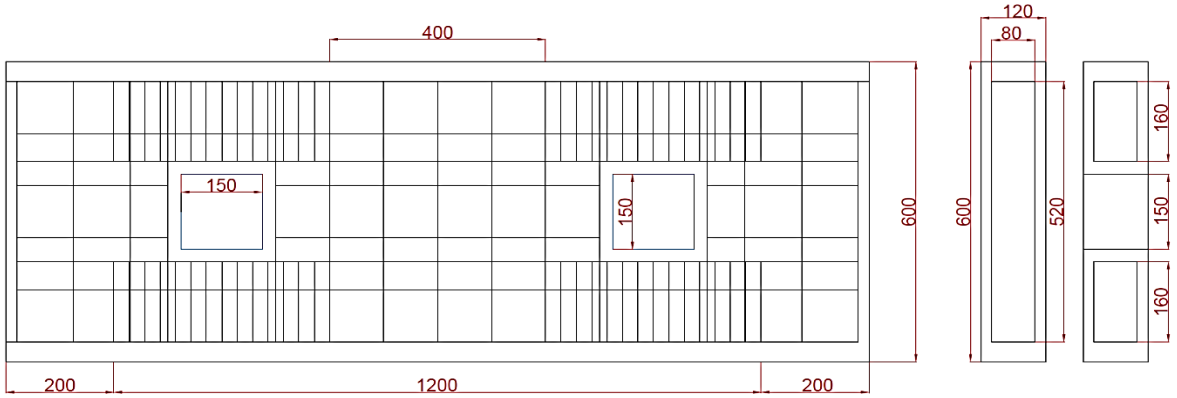

Fig 7: Structural detailing of HMT by Ibrahim et al. [1] and utilized to develop DEO (All dimensions are in mm)

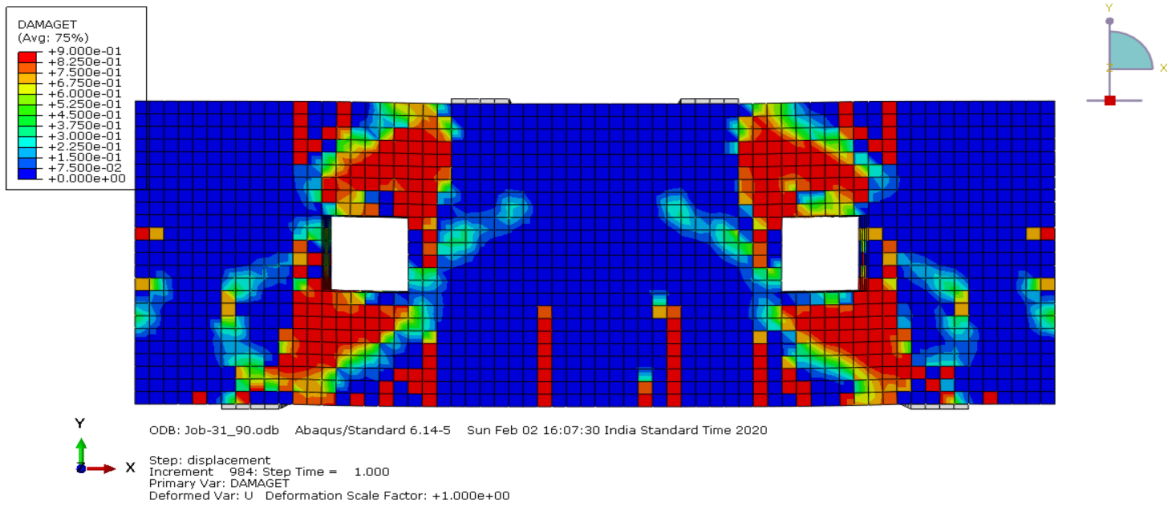

Fig 8: FEM tension damage of DEO

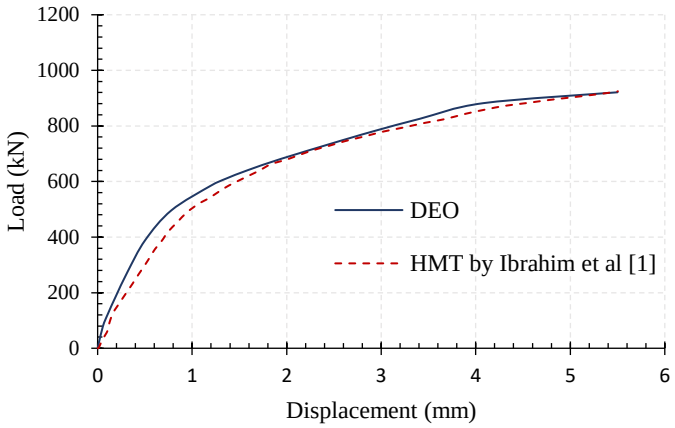

Fig 9: Load vs. displacement graph of HMT (HSC deep beams with medium opening) by Ibrahim et al. and DEO (replication of work carried out in present study for verification)

Table VIII: Comparison between analytical results obtained by Ibrahim et al. [1] and present study using ABAQUS program

P_u (kN)			Deflection at ultimate load Δ(mm)		
$P_{Ibrahim\ et\ al.\ [1]}$	$P_{Present\ study}$	$P_{Ibrahim\ et\ al.\ [1]} / P_{Present\ Study}$ (%)	$\Delta_{Ibrahim\ et\ al.\ [1].}$	$\Delta_{Present\ Study}$	$\Delta_{Ibrahim\ et\ al.\ [1]} / \Delta_{Present\ Study}$ (%)
462	460.5	99.67	5.5	5.5	100

The Load vs. Displacement curves exhibit remarkable similarity between the HMT and DEO models, as depicted in Fig. 9. Analysis of Table VIII reveals that the finite element (FE) model employed in this study precisely replicated the ultimate loads of deep beams with shear openings documented by Ibrahim et al. [1]. The average ratio of ultimate loads stood at 99.67%, showcasing a minimal difference of 1.76% in energy absorption capacity. This outcome underscores the efficacy of the utilized FE model for simulating deep beams with openings, offering substantial potential for further research and extension studies.

4. ADEQUACY OF THE PROPOSED STEEL CONFIGURATIONS

This study encompasses the simulation of four distinct models, each engineered to enhance performance, particularly in shear strength. Model OEB involves the introduction of a 130 mm diameter opening in an existing solid deep beam, aimed at accommodating utilities and assessing the resultant loss in shear strength, as illustrated in Fig. 10(i). In Model EDSPO, eight rectangular plates measuring 300×150×5 mm are affixed on either side of the beam, secured with ten 10 mm diameter bolts, as depicted in Fig. 10(ii). Additionally, both Models EDSBPB and EDSBPD integrate an external Φ130 mm steel cylinder with a 5 mm thickness. EDSBPB incorporates four steel plates of 200×200×5 mm assembled with four bolts, while EDSBPD employs ten steel bolts to connect four steel plates of 200×500×5 mm, outlined in Fig. 10(iii) and (iv). Comprehensive details of these models, including the proposed steel configurations, are visually represented in Fig. 10.

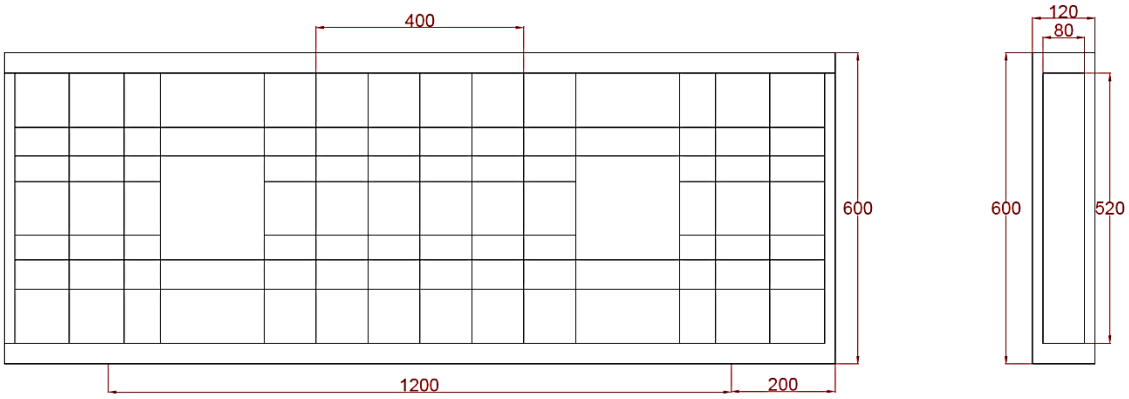

i. OEB

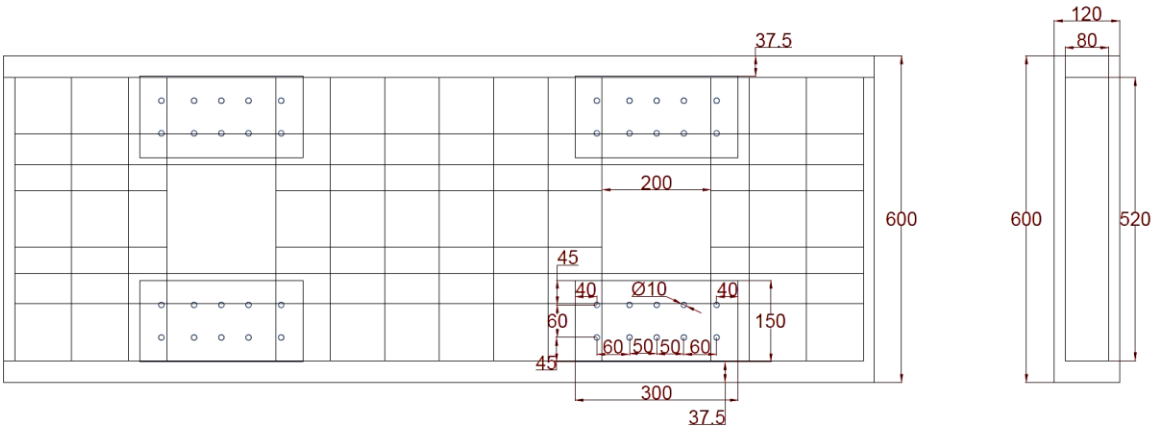

ii. EDSPO

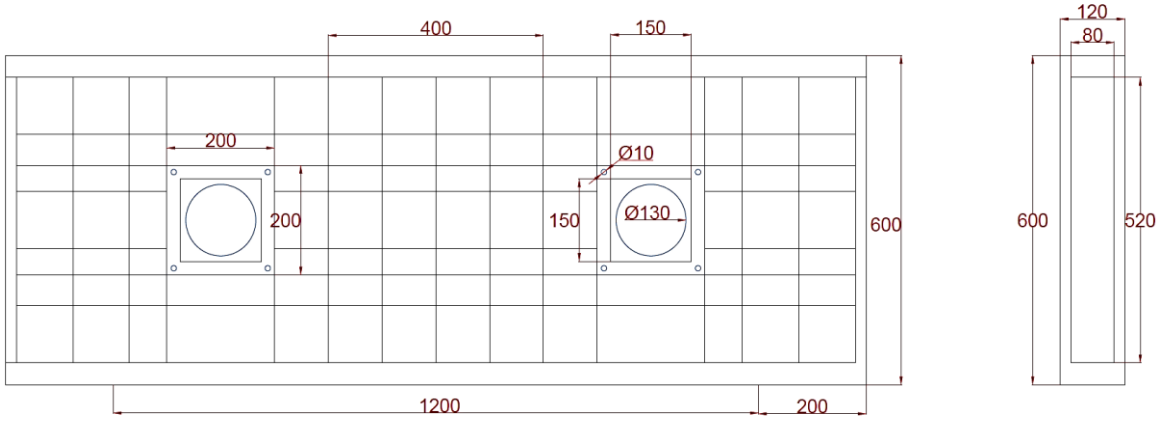

iii. EDSBPB

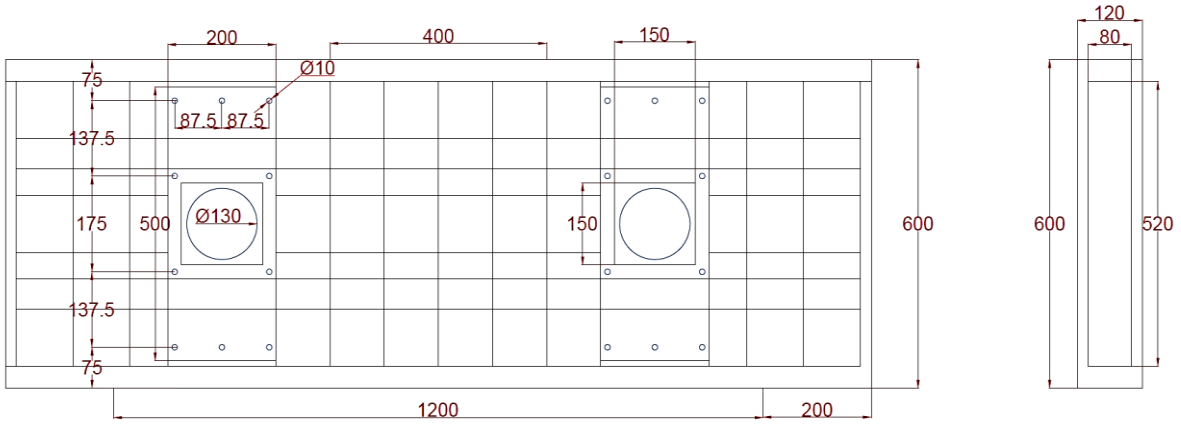

iv. EDSBPD

Fig 10: Structural detailing of all models incorporating steel configurations around opening (All dimensions are in mm)

In the realm of structural interaction, tie constraints are meticulously designated to assemble the intricate steel configurations enveloping the openings in beams EDSBO, EDSBPB, and EDSBPD. Here, a master-slave relationship is established, designating the steel's contact surface as the master and the opening surface (comprising concrete) as the slave. The connection of bolts is facilitated through a surface-to-surface contact interaction protocol (standard), wherein the bolt's contact surface serves as the master, engaging with the inner surface of concrete holes designated as the slave surface. A comprehensive analysis of DAMAGET values across all models, illustrating the intricate crack patterns surrounding the openings, is meticulously presented in Fig. 11.

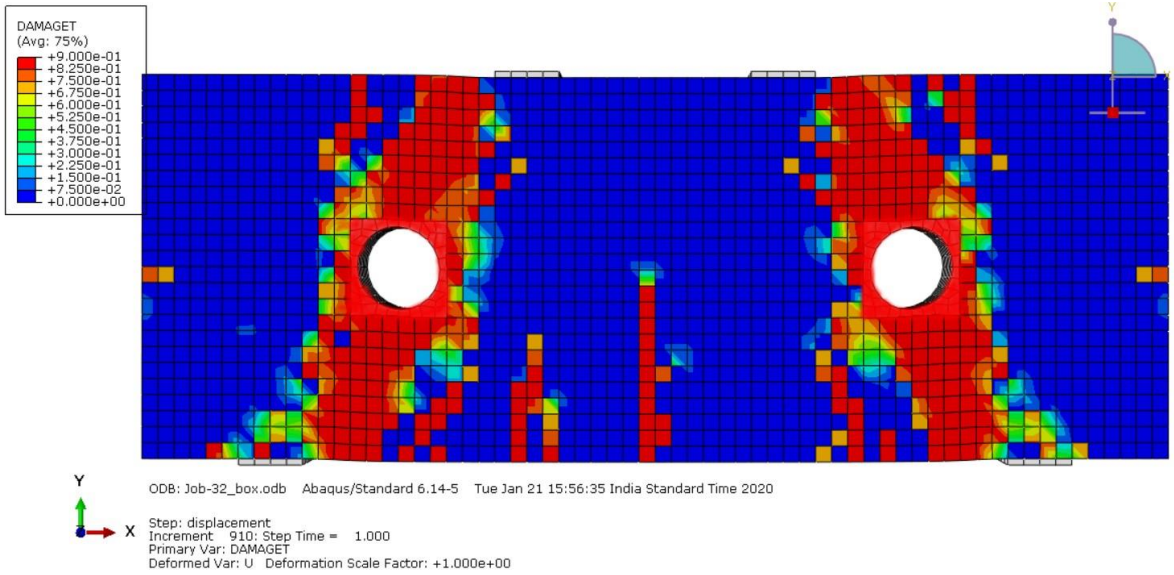

i. OEB

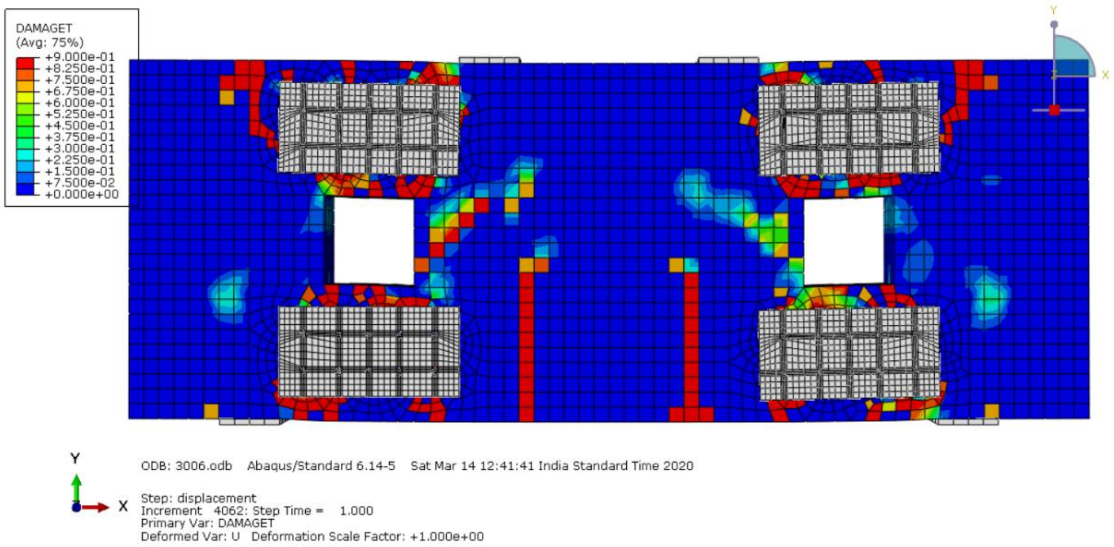

ii. EDSPO

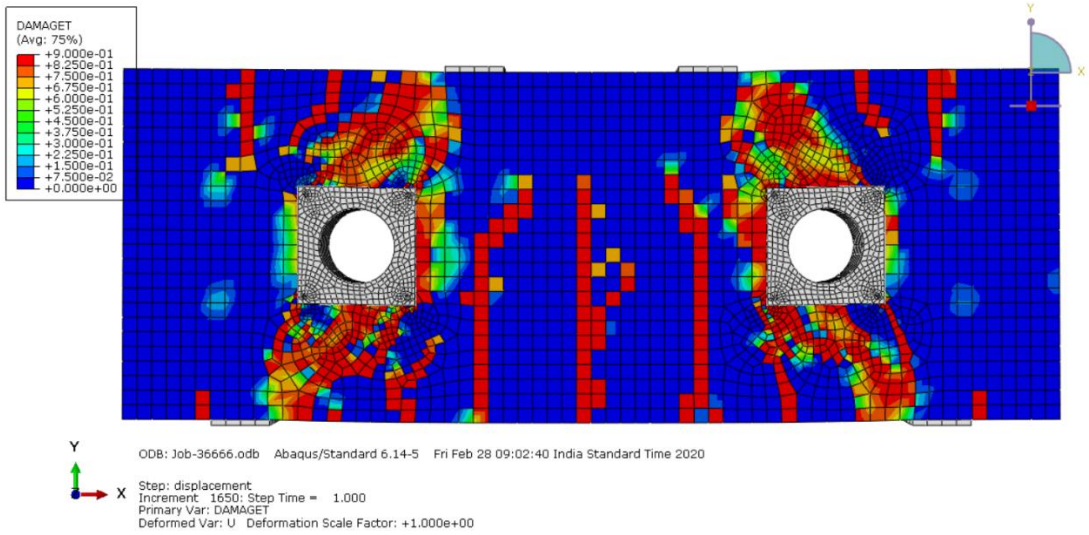

iii. EDSBPB

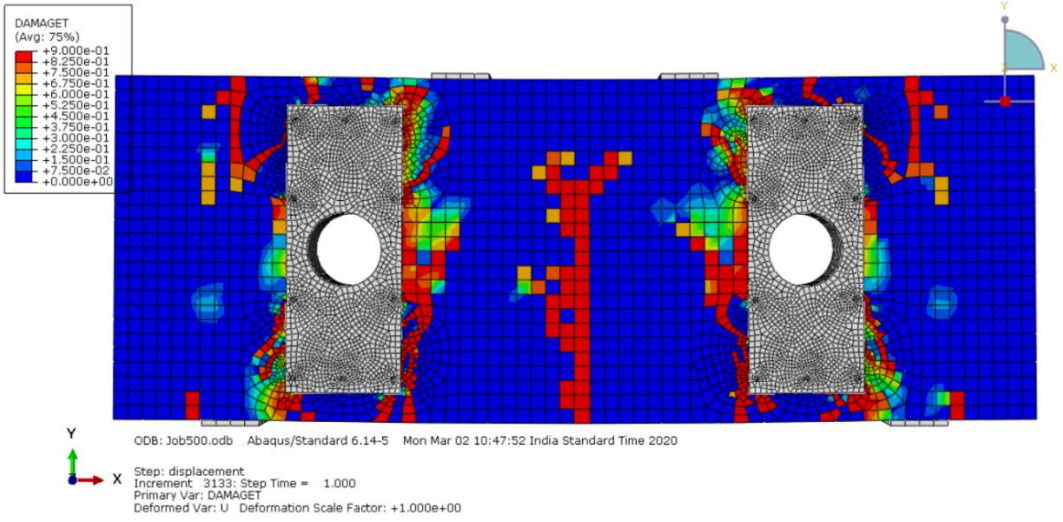

iv. EDSBPD

Fig 11: Crack pattern and tensile damage of deep beam with proposed steel configurations.

The propagation of cracks within the simulated prototype is attributed to the tensile stresses exerted. It is evident that the strategic integration of steel configurations surrounding the openings enhances the efficiency of the deep beam significantly, effectively curbing the development of excessive cracks. Detailed stress values within the proposed steel configurations and reinforcements are meticulously depicted, providing valuable insights, as presented in Fig. 12.

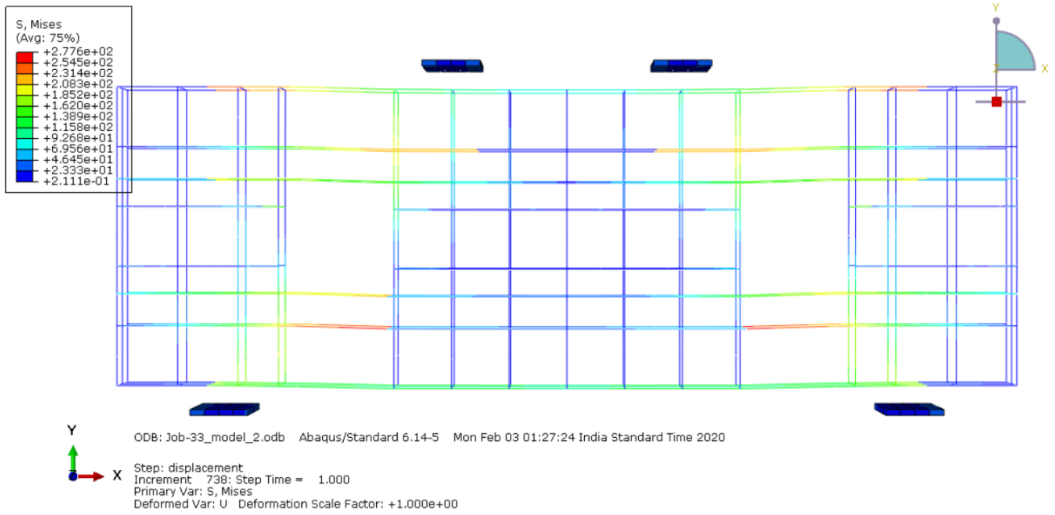

i. OEB

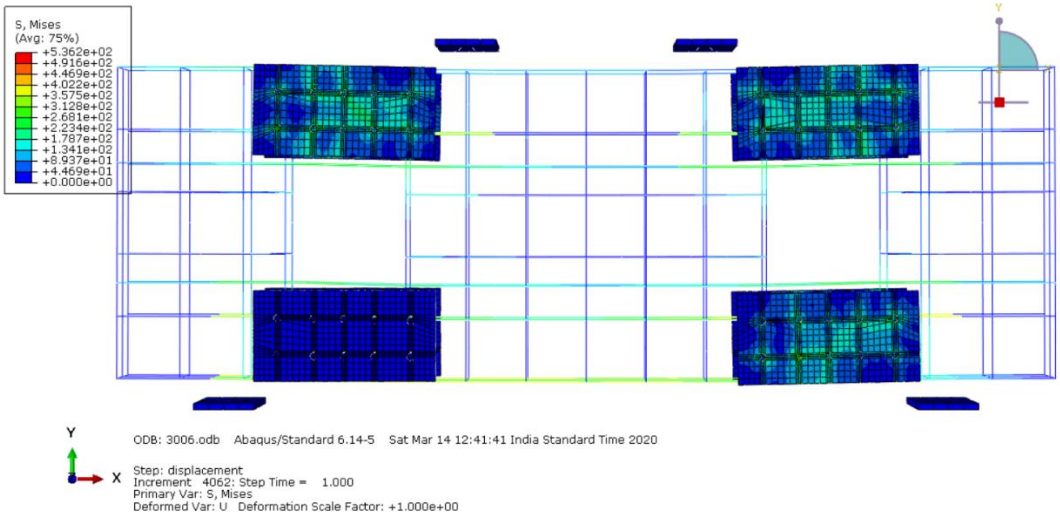

ii. EDSPO

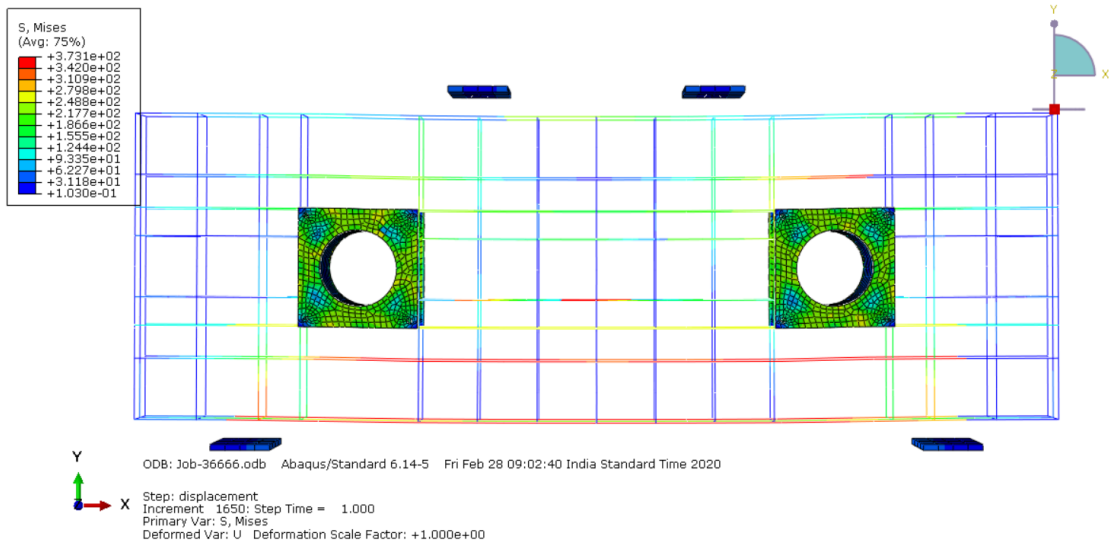

iii. EDSBPB

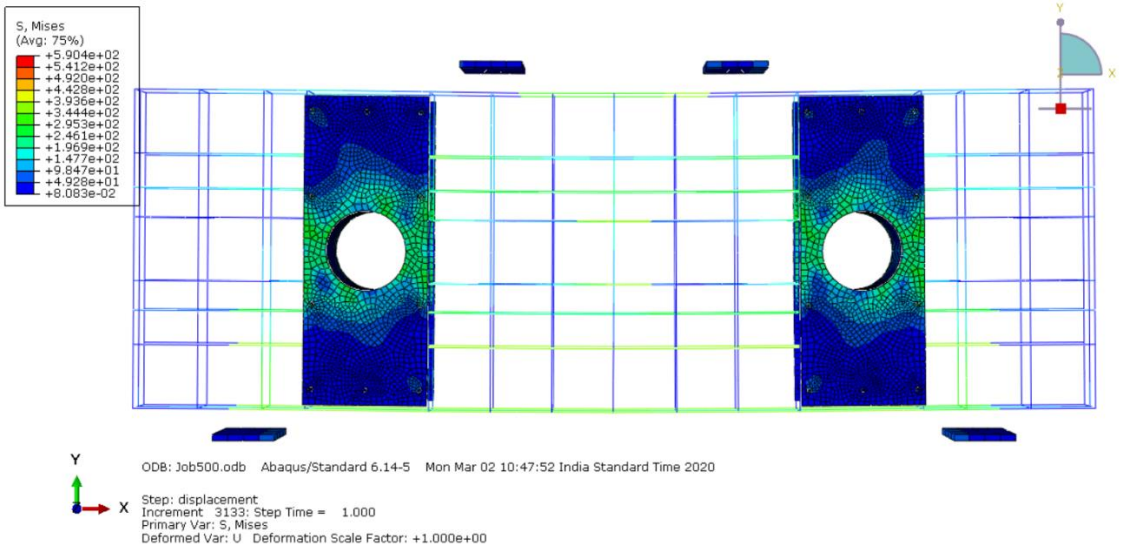

iv. EDSBPD

Fig 12: Stresses in the proposed steel configurations and reinforcements for deep beams OEB, EDSPO, EDSBPB, and EDSBPD

Upon comparison of Fig. 11 and 12, it becomes apparent that the EDSBPD and EDSBPB configurations, acting as external steel assemblies, effectively bear the shear stresses without inducing excessive crushing of concrete around the shear opening up to its ultimate loading capacity. Notably, the transfer of stress to the proposed steel configurations leads to diminished crack propagation, enhancing the load-carrying capacity of the deep beam. Consequently, these configurations can be strategically designed to regain strength after the provision of cutouts.

A. Efficiency of proposed steel configurations

The Load vs. Displacement graph comparisons for all beams, as illustrated in Fig. 13, reveal a significant reduction in load-carrying capacity of existing deep beams upon creating an opening in the shear zone, aligning with the findings of Ibrahim et al [1] and previous studies. However, the configurations implemented in models EDSBPB and EDSBPD exhibit efficiency in enhancing the load-carrying capacity, restoring the deep beam to its full strength even after the introduction of an opening. This enhanced performance is attributed to the uniform distribution of stresses facilitated by external provisions. A detailed presentation of all obtained results is provided in tabular format in accordance with Table IX.

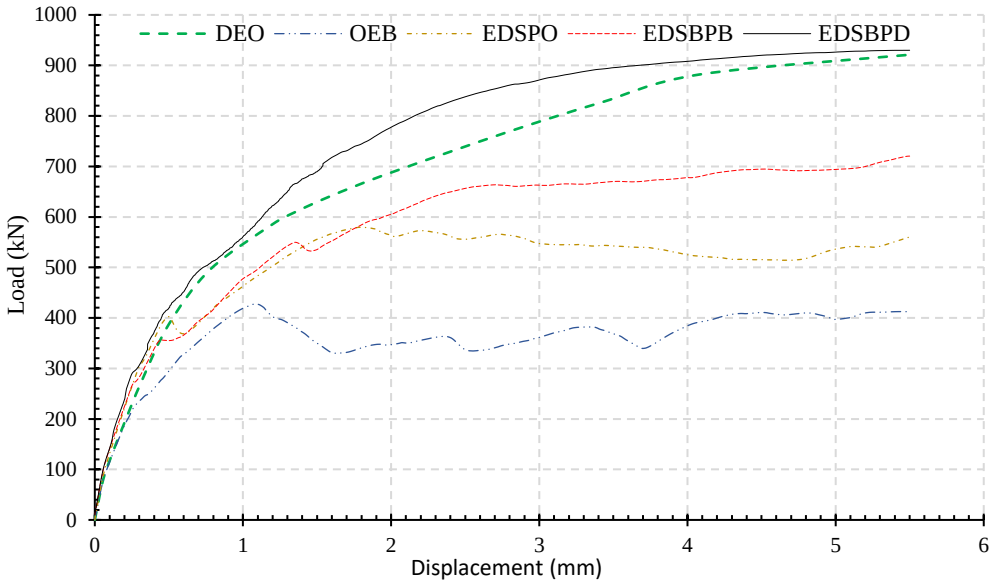

Fig 13: Load vs. Displacement graph of all models

Table IX: Test results of all proposed steel configurations

Model	FEM Load (kN)	Area Under the Curve (kN.mm)	Shear strength relative to solid deep beam (P_o/P_s)
OEB	206.02	1969.94	0.4459
EDSPO	289.8	2141.92	0.6272
EDSBPB	360.13	3175.58	0.7795
EDSBPD	464.96	4173.52	1.0064
*FEM Solid Deep Beam's ultimate load result recorded as 462 kN (Ps) and ACI 318-14 ultimate load 394 kN			
**h is limited to 0.3d × 0.5a, f'c is 50 MPa, Area of opening is 13273.23mm^2, Area of shear zone (a*d) is 240000mm^2, and Ao/Asz ratio is 0.055 considered for parametric study.			

5. PARAMETRIC STUDY

In the process of rehabilitating the shear strength of deep beams with shear openings, a crucial prerequisite is understanding the provisions utilized in the design of analogous solid deep beams. This parametric study adhered to the guidelines outlined in ACI 318-14 [1] for the preliminary sizing and design of the solid deep beams, ensuring compliance with all specified requirements. The results of the study, specifically the shear capacity variations concerning different widths and thicknesses of the steel configurations, are tabulated in Table X.

Table X: Shear capacity of EDSBPD accounting variable thickness and width of steel configuration

w_s (mm)	t_s (mm)	t_s / w_s	Ultimate load P_o (kN)	Shear strength relative to solid deep beam P_o/P_S
200	2	0.01	420.21	0.9125
	4	0.02	445.89	0.9694
	6	0.03	470.08	1.0208
	8	0.04	495.71	1.0819
	10	0.05	518.50	1.1260
250	2	0.008	432.10	0.9383
	4	0.016	460.00	0.9989
	6	0.024	485.23	1.0537
	8	0.032	508.74	1.1048
	10	0.04	530.07	1.1511
300	2	0.00667	443.12	0.9623
	4	0.01333	465.34	1.0105
	6	0.02	489.56	1.0631
	8	0.02667	514.91	1.1182
	10	0.03333	535.64	1.1632
350	2	0.00571	451.14	0.9797
	4	0.01143	475.06	1.0316
	6	0.01714	499.00	1.0836
	8	0.02286	523.14	1.1360
	10	0.02857	546.62	1.1870
400	2	0.005	458.14	0.9949
	4	0.01	483.46	1.0499
	6	0.015	508.23	1.1036
	8	0.02	530.82	1.1527
	10	0.025	552.34	1.1994
*h is limited to 0.3d × 0.5a, f'c is 50 MPa, Area of opening is 13273.23mm^2, Area of shear zone (a*d) is 240000mm^2, and A_o/A_{sz} ratio is 0.055 considered for parametric study. **FEM Solid Deep Beam's ultimate load result recorded as 462 kN (P_s) and ACI 318-14 ultimate load 394 kN				

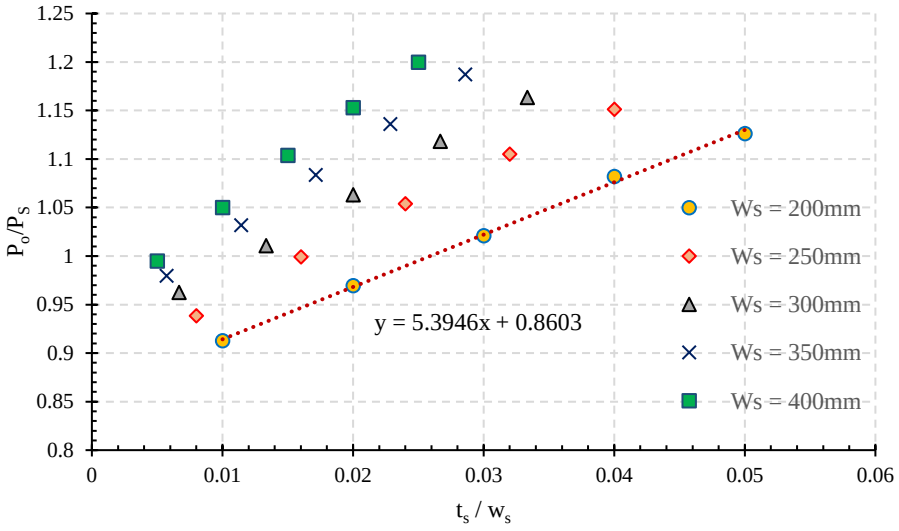

Fig 14: Relationship between ultimate load capacity and the plate size ratios (A_o/A_s = 0.055)

Figure 14 presents an X-Y plot demonstrating the relationship between parameters. The Y-axis signifies the ratio of the load capacity of deep beams with varying opening sizes to the load capacity of solid deep beams. On the X-axis, the ratio between the thickness and width of the steel plate integrated into the shear zone opening is depicted. The lower bound of this relationship can be mathematically represented as y = 5.3946x + 0.8603, where y represents P_o/P_s and x represents t_s/w_s. When substituting the parameters into the equation, it takes the form:

$$\frac{P_O}{P_S} = 5.3946 \frac{t_S}{w_S} - 0.86 \quad (7)$$

This equation serves as a predictive tool for estimating the ultimate load-bearing capacity of deep beams with steel configurations around shear zone openings relative to the strength of solid deep beams. Here, P_s and P_o represent the shear strength of the solid beam and deep beam with steel configurations at openings, respectively. P_s is replaced with the shear strength of the deep beam, denoted as $V_n = 0.83\sqrt{f'c}$ b d, following the guidelines in ACI 318-14 [1].

The derived dimensionless formula is as follows:

$$V_n = 0.83\sqrt{f'c}\ b\ d\ \left(5.3946 \frac{t_S}{w_S} - 0.86\right) \quad (8)$$

It is imperative to note that this equation is applicable to any deep beams with shear openings sharing the same shear span-to-depth ratio (a/d) of 0.67. However, it is restricted to openings with a specific area ratio (A_o/A_{sz}) of 0.055. For diverse a/d ratios and variable A_o/A_s ratios, additional formulas need to be derived to provide comprehensive design assistance.

6. Conclusions

- Comparative analyses displayed a substantial increment in ultimate load carrying capacity by 20% in EDSPO, 36% in EDSBO, 72% in EDSBPB, and a distinct 101% in EDSBPD concerning the base case of solid deep beam. Additionally, energy absorption capacity demonstrated a remarkable 6% increase in EDSBPD, contrasting with 43% reduction in OEB, 37% in EDSPO, 8% in EDSBPB compared to DEO.
- It is observed by comparing OEB with DEO, 52% reduction in ultimate load after providing opening in existing deep beam and satisfied the shear strength of deep beam according to ACI 318-14 [14] , which is $V_n = 0.83\sqrt{f'c}$ b d .
- EDSBPD demonstrates superior crack control around the shear opening compared to EDSBPW, as evidenced by the detailed analysis conducted through DAMAGET assessments.

- The devised empirical equation (Equation 8) provides a robust predictive tool, enabling engineers to estimate the ultimate load-bearing capacity of deep beams with steel configurations around shear zone openings. This equation, rooted in the principles of ACI 318-14 and the interplay between steel plate dimensions and opening characteristics, offers a valuable framework for designing deep beams with openings, allowing for precise calculations while adhering to industry standards.
- Furthermore, the study highlights the need for additional formulations to accommodate different shear span-to-depth ratios (a/d) and variable area ratios of openings to shear zones (A_o/A_{sz}). This emphasizes the importance of further research to expand the applicability of these findings across a broader range to optimize structural configurations.

REFERENCES

[1] Ibrahim M.A., Thakeb A. El., Mostfa A.A. and Kottb H.A. (2018). "Proposed formula for design of deep beams with shear openings." "Housing and Building National Research Center", Vol. 14, pp. 450-465

[2] Wahalathantri B.L., Thambiratnam D.P., Chan T.H.T. and Fawzia S. (2011). "A material model for flexural crack simulation in reinforced concrete elements using ABAQUS." "Faculty of built environment and engineering, Queensland University of Technology", pp. 260-264

[3] Mohamed Ashraf Ragab, Shoukry Mohie S. and Saeed Janet M. (2014). "Prediction of The Behavior of Reinforced Concrete Deep Beams with Web Openings Using the finite element method." "Alexandria Engineering Journal", Vol. 53, pp. 329–339

[4] Hafezolghorani Milad, Hejazi Farzad, Vaghei Ramin, Saleh Bin Jaafar Mohd and Prof. Karimzade Keyhan. (2017). "Simplified Damage Plasticity Model for Concrete." "Structural Engineering International", Vol. 27, pp. 68-78

[5] Abaqus Analysis User's Manual – Abaqus version 6.10 (2016) along year 2017 at http://abaqusdoc.ucalgary.ca/books/usb/default.htm?startat=pt05ch21s02abm42.html.

[6] Dr. Ibrahim M. A., Dr. Thakeb A. El., Prof. Dr. Mostafa A. A. and Eng. Kottb H. A. (2018). "Experimental study of new reinforcement details for reinforced concrete deep beams with shear opening." "Al-Azhar University of Civil Engineering Research Magazine (CERM)", Vol. 40, pp. 347-367

[7] Bose Jithin K J, Thomas Job and Parappattu Nidhin B. (2016). "Effect of Openings in Beams – A Review." "International Journal of Innovative Research in Advanced Engineering", Vol. 9, pp. 15-19

[8] ECP 203-2007: "Egyptian Code of Practice." "Design and construction for reinforced concrete structures." "Ministry of Building Construction, Research Center for Housing, Building and Physical Planning", Cairo, Egypt, 2007

[9] Grassl, P., Xenos, D., Nyström, U., Rempling, R., & Gylltoft, K. (2013). CDPM2: A damage-plasticity approach to modelling the failure of concrete. International Journal of Solids and Structures, 50(24), 3805–3816. doi:10.1016/j.ijsolstr.2013.07.00

[10] ACI Committee 318. Building Code Requirements for structural concrete (ACI 318-14) and commentary (318R-14). Farmington Hills, MI: American Concrete Institute; 2014. p. 524.

[11] G. Campione, G. Minafò, Behavior of concrete deep beams with openings and low shear span-to-depth ratio, Eng. Struct. 41 (3) (2012) 294–306.

[12] W.E. El-Demerdash et al, Behavior of RC shallow and deep beams with openings via the strut-and-tie model method and nonlinear finite element, Arab. J. Sci. Eng. 41 (2) (2016) 401–424.

[13] R. Nayal, H.A. Rasheed, Tension stiffening model for concrete beams reinforced with steel and FRP bars, J. Mater. Civil Eng. 19 (6) (2006) 831–841.

[14] E. Hognestad, A study of combined bending and axial load in reinforced concrete members, Univ. Illinois Bull. 49 (1951) (22).

[15] Yang et al, The influence of web openings on the structural behavior of reinforced high-strength concrete deep beams, Eng. Struct. 28 (13) (2006) 1825–1834.